OXFORD

REGULAR RESEARCH ARTICLE

Small Extracellular Vesicles in Rat Serum Contain Astrocyte-Derived Protein Biomarkers of Repetitive Stress

Cristóbal Gómez-Molina, Mauricio Sandoval, Roberto Henzi, Juan Pablo Ramírez, Manuel Varas-Godoy, Alejandro Luarte, Carlos Andres Lafourcade, Alejandra Lopez-Verrilli, Karl-Heinz Smalla, Thilo Kaehne, Ursula Wyneken

Centro de Investigación Biomédica, Universidad de los Andes, Chile (Mr Gómez-Molina and Drs Sandoval, Henzi, Ramírez, Varas-Godoy, Luarte, Lafourcade, Lopez-Verrilli, and Wyneken); Leibniz Institute for Neurobiology, Magdeburg, Germany (Dr Smalla); Otto-von-Guericke University, Magdeburg, Germany (Dr Kaehne).

Correspondence: Ursula Wyneken, Laboratorio de Neurociencias, Centro de Investigación Biomédica, Facultad de Medicina, Universidad de los Andes; Mons. Alvaro del Portillo 12.455, Las Condes; Santiago, Chile (uwyneken@uandes.cl).C.G.-M. and M.S. contributed equally to this work

Abstract

Background: Stress precipitates mood disorders, characterized by a range of symptoms present in different combinations, suggesting the existence of disease subtypes. Using an animal model, we previously described that repetitive stress via restraint or immobilization induced depressive-like behaviors in rats that were differentially reverted by a serotonin- or noradrenaline-based antidepressant drug, indicating that different neurobiological mechanisms may be involved. The forebrain astrocyte protein aldolase C, contained in small extracellular vesicles, was identified as a potential biomarker in the cerebrospinal fluid; however, its specific origin remains unknown. Here, we propose to investigate whether serum small extracellular vesicles contain a stress-specific protein cargo and whether serum aldolase C has a brain origin.
Methods: We isolated and characterized serum small extracellular vesicles from rats exposed to restraint, immobilization, or no stress, and their proteomes were identified by mass spectrometry. Data available via ProteomeXchange with identifier PXD009085 were validated, in part, by western blot. In utero electroporation was performed to study the direct transfer of recombinant aldolase C-GFP from brain cells to blood small extracellular vesicles.
Results: A differential proteome was identified among the experimental groups, including aldolase C, astrocytic glial fibrillary acidic protein, synaptophysin, and reelin. Additionally, we observed that, when expressed in the brain, aldolase C tagged with green fluorescent protein could be recovered in serum small extracellular vesicles.
Conclusion: The protein cargo of serum small extracellular vesicles constitutes a valuable source of biomarkers of stress-induced diseases, including those characterized by depressive-like behaviors. Brain-to-periphery signaling mediated by a differential molecular cargo of small extracellular vesicles is a novel and challenging mechanism by which the brain might communicate health and disease states to the rest of the body.

Keywords: exosomes, stress subtypes, biomarkers

Significance Statement

We previously reported that different stress types are able to induce depressive-like behaviors in rats, which are selectively sensitive to pharmacological treatments. Here, investigated whether such difference among stress types and pharmacological sensitivity are associated with possible protein biomarkers in the peripheral blood, present in small extracellular vesicles (sEVs). After stress by movement restriction (restraint in cages or immobilization in bags), a stress-specific proteome was detected in serum sEVs. Moreover, a recombinant protein expressed selectively in brain cells was detected in blood sEVs. Our results show that brain-derived sEVs may constitute a pathway of brain-to-periphery communication and a relevant source of biomarkers for central nervous system diseases.

Introduction

Chronic stress precipitates depressive states in humans and induces depressive-like behaviors in animal models of mood disorders. However, mood disorders in patients comprise heterogeneous subgroups with different underlying pathophysiological mechanisms (Krishnan and Nestler, 2010) (Akil et al., 2018). Currently, it is clear that different biological networks and signaling systems contribute to the expression of depressive-like behaviors, an issue that highlights the complexity of recapitulating the disease or even more, of disease subgroups, in animal models (Darcet et al., 2016). We established an animal model of stress using rats exposed to repetitive stress by movement restriction either by restraint in small cages or immobilization in plastic bags (Ampuero et al., 2015). In these animal models, depressive-like behaviors were selectively reverted by antidepressant drugs acting on either serotonin- or noradrenaline-mediated neurotransmission (i.e., fluoxetine and reboxetine, respectively), suggesting neurobiological differences among both stress paradigms. In addition, these experimental groups differed in their body weight gain and sucrose preference after 10 days of stress. Moreover, the glycolytic enzyme aldolase C that is expressed in CNS astrocytes, as well as in Purkinje neurons in the cerebellum, was detected in small extracellular vesicles (sEVs) isolated from cerebrospinal fluid (CSF) at high levels after restraint but not after immobilization, indicating that stress by movement restriction applied with 2 different procedures generates differential physiological or molecular responses. Several types of extracellular vesicles (EVs), secreted by cells, are involved in cell-to-cell communication (Sandoval et al., 2013; Colombo et al., 2014; Pegtel et al., 2014). They comprise vesicles directly released from the plasma membrane and vesicles termed exosomes, which are generated in the endocytic pathway and are released from multi-vesicular bodies. Exosomes are defined by their small size (<150 nm) and their particular biogenesis pathway, but when they are isolated by ultracentrifugation a mixed population of EVs is obtained, which are now better termed "small EVs" (Kowal et al., 2016). The identification of their molecular content, including proteins, has gained an increasing amount of interest as disease biomarkers (Shao et al., 2012). Considering that translational relevant biomarkers should be obtained from a more accessible sample than the CSF, we performed proteomic analysis of serum-derived sEVs of rats exposed to stress by restraint or immobilization. Moreover, serum sEVs contained aldolase C tagged with green fluorescent protein (C-GFP), used as a reporter protein in forebrain cells including astrocytes, revealed that brain-derived proteins can be found in blood sEVs.

Methods

Animals

Male Sprague–Dawley rats between 2.5 and 3 months of age were used for the stress protocols. To transfer aldolase C-GFP via in utero electroporation, pregnant rats were used. The progeny grew until young adulthood, and their blood was obtained. The experimental procedures were supervised and approved by the Universidad de los Andes Bioethical Committee, and the National Institute of Health's Guide for the Care and Use of Laboratory Animals was followed. Rats were maintained with ad libitum access to food and water under a 12-h-light/-dark cycle at 22°C ±1°C.

Experimental Design

The stress procedures used were described previously and applied as in Figure 1A (Ampuero et al., 2015). During a 7-day habituation period, 4 to 5 male rats were housed in home cages. Then the rats were exposed to stress due to movement restriction for 2 h/d (9 to 11 AM) over 10 consecutive days, and they spent the rest of the day in their home cages. Both no stress as well as stress groups were water and food deprived during these 2 hours. The no stress rats were handled at least twice for 5 minutes during this time and were subjected to deprivation to control for direct effects of deprivation and handling. Movement restriction was attained either by restraint in wire mesh cages or by immobilization in plastic bags. On day 11, that is, 24 hours after the beginning of the last stress session, the blood was collected and serum obtained by centrifugation at $4000 \times g$ for 10 minutes and kept refrigerated until further centrifugation for EVs isolation. The complete behavioral characterization on day 11 is published in Ampuero 2015. Rats of the present experimental groups were weighted on day 1 (before initiation of the stress session) and on day 11 to calculate body weight gain. The sucrose preference test was also performed. For this, during the habituation period and previous to the initiation of the stress protocol, rats chose between drinking 1% sucrose or tap water during 3 consecutive days. After the last stress procedure, rats were water deprived for 12 hours (i.e., on day 10) and sucrose intake was measured for 1 hour on day 11 (Supplementary Figure 1).

In Utero Electroporation

Electroporation was performed from embryonic stage E18.5 to 19.5, thus preferentially targeting astrocytes (Ampuero et al., 2015). To anesthetize pregnant rats, xylazine (5 mg/kg) and ketamine (50 mg/kg) were administered via i.p. injection. Uterine horns were exposed and plasmid mixtures (2.7 µg of each plasmid mixed with 0.5 µL of Fast Green [1 mg/mL, Sigma-Aldrich]) were injected into the left lateral ventricle using pulled glass capillaries (P97, Sutter Instruments) connected to a pressure Pico pump (PV830, World Precision Instruments). The plasmids were pPBGFAP-PBase (approximately 2 µg/µL), that is, driven by the glial fibrillary acid protein (GFAP) promoter combined with: (1) pBCAG-AldoC-GFP (approximately 2 µg/µL), that is, driven by the
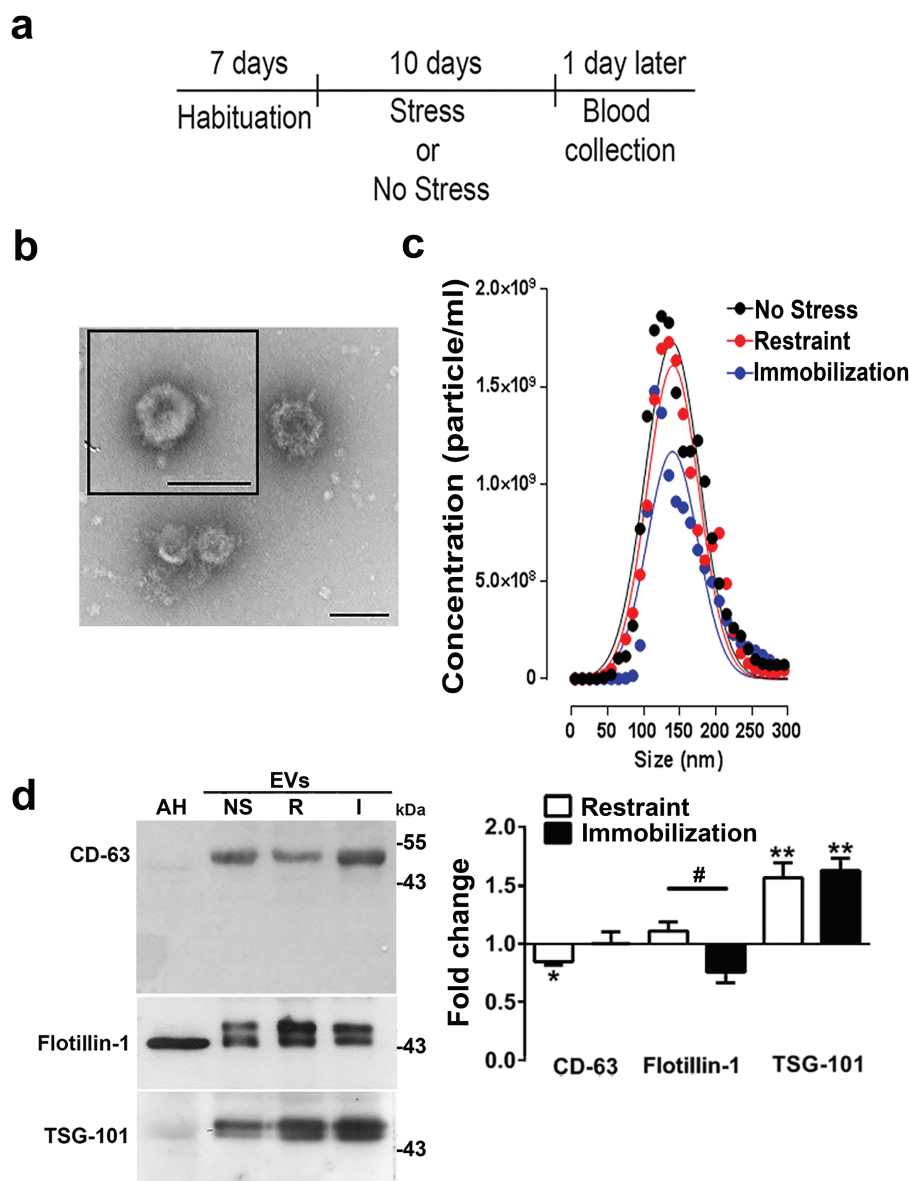
Figure 1. Characterization of small extracellular vesicles (sEVs). (a) Experimental design: rats were habituated in their home cages for 7 days. Then, stress by restraint or immobilization or no stress was applied for 10 days. (b) Images of sEVs obtained by electron microscopy. Bar scale = 100 nm. (c) sEV size and concentration detected by the nanoparticle tracking analysis in 4 to 6 independent samples per animal group. (d) Western blots and (e) the corresponding densitometric quantification of changes in the content of the indicated proteins in the experimental conditions: no stress (NS), restraint (R), or immobilization (I). Equal amounts of proteins were loaded per lane (including astrocyte homogenates, AH). The data represent mean±SEM. n=10 for CD-63, n=8 and 5 for flotillin after restraint and immobilization, respectively; n=7 for TSG-101. #$P<.05$ in the Mann-Whitney test (used to compare pairs of data, i.e., restraint vs immobilization). *$P<.05$, **$P<.01$ in a Wilcoxon-signed rank test (to compare with a hypothetical value of 0 (no change).

strong ubiquitous promoter cytomegalovirus early enhancer/chicken beta actin; or (2) pBCAG-GFP (approximately 2 μg/μL) (used as control). The pPBGFAP-PBase and pBCAG-GFP plasmids were kindly donated by Joseph LoTurco and were allowed through the piggyBac transposon system, a stable transgene expression in astrocyte progenitors (LoTurco et al., 2009; Chen and LoTurco, 2012). For electroporation, a 60- to 70-V electric pulse was delivered across a pair of oval electrodes (1×0.5 cm) with the positive pole placed on the lateral surface of the left cerebral hemisphere. Finally, the electroporated fetuses were born and grew until young adulthood (2.5–3 months) for collection of brain samples for immunofluorescence and for blood collection (Figure 4A).

Immunohistofluorescence

Electroporated rats of 250 g were anesthetized with ketamine (50 mg/kg) and xylazine (5 mg/kg) and were perfused intra-cardially with 0.9% saline followed by 4% paraformaldehyde. Then the brains were removed, cryopreserved, and cut in 30-μm frozen coronal sections using a Microm HM 525 cryostat (Thermo Fisher Scientific). Serial sections from electroporated and nonelectroporated rats were incubated with blocking solution (phosphate buffered saline [PBS] pH=7.4, 0.25% w/v Triton X-100, 5% w/v horse serum [#16050130, Gibco-Invitrogen, San Diego, CA], 5% w/v bovine serum albumin [BSA]) for 1 hour at room temperature. Then they were incubated overnight at 4°C with the

corresponding primary antibodies (anti-GFAP and anti-GFP) diluted to 1:1000 with PBS pH 7.4, 0.25% w/v Triton X-100, 1% w/v horse serum, and 1% w/v BSA. Then the sections were incubated for 1 hour at room temperature with diluted (1:1000) secondary antibody coupled to fluorescent probes (Alexa anti goat 488 or Alexa anti mouse 555). Omission of the primary antibody during incubation was used as control. Slides were cover slipped by using Vectashield mounting medium (Dako, Agilent) and inspected under an epifluorescence microscope (Nikon, ECLIPSE TE2000U) or a confocal microscope (Leica SP8) to study co-localization by using the multidimensional acquisition software.

Isolation of sEvs

Approximately 6 mL of blood was obtained per rat to follow the procedure of Thery et al., 2006. Serum was centrifuged at $2000 \times g$ for 30 minutes to discard cells and at $12\,000 \times g$ for 45 minutes to discard microvesicles. The resulting supernatant was centrifuged at $110\,000 \times g$ for 70 minutes to collect the sEV-enriched fraction. sEVs were washed once in PBS and centrifuged as before to resuspend the final pellet in PBS and store it at –80°C.

Western Blots

A BCA protein assay kit (Pierce) was used to measure protein concentrations. Polyacrylamide gradient gel electrophoresis (4%–20%) in denaturing conditions (sodium dodecyl sulfate polyacrylamide gel electrophoresis [SDS-PAGE]) was used to separate 20 µg of protein per lane and to transfer them thereafter to nitrocellulose membranes. As a positive control for the exosomal proteins, astrocyte primary culture homogenates, suspended in RIPA buffer [(0.1% SDS, 0.5% NP40, 10 mM Tris-Cl pH 7.5, 1 mm EDTA, 150 mM NaCl, 0.5% deoxycolate plus protease inhibitor cocktail (Complete, Sigma-Aldrich)], was used. Astrocyte primary cultures were routinely obtained in our laboratory on day P1 (Sandoval et al., 2013). Exosomal proteins, suspended in PBS, were used. Antibodies used in western blots are listed below.

Immunoprecipitation

The procedure was performed at 4°C. sEV proteins (250 µg) were solubilized in RIPA buffer for 2 hours. The primary antibodies (goat aldolase C from Santa Cruz or mouse small ubiquitin-like modifier (SUMO) 1 from Cell Signaling) or the corresponding control immunoglobulin IgG were added to the supernatants and incubated overnight to finally add 100 µL of washed and blocked protein G Sepharose beads for 1 hour. The supernatant was discarded after centrifugation at 500 g, and the beads were washed 5 times with solubilization buffer. Finally, the beads were incubated with electrophoresis loading buffer for western-blot analyses.

Isolation of EAAT2-Positive sEVs

sEVs (250 µg per tube) were diluted in 1 mL of iso-osmotic buffer (0.32 M sucrose, 50 mM HEPES, pH 7.4) and incubated overnight at 4°C with anti-EAAT2 antibody directed against an epitope located at the second extracellular loop of the rat Excitatory Amino Acid Transporter 2 (tube A). As negative control, normal rabbit serum was used. In parallel, 100 µL of Dynabeads M-280 Sheep anti-rabbit IgG (Life Technologies, Darmstadt, Germany) was pelleted using a magnet for 5 minutes. The supernatant was discarded and the magnetic beads were washed 2 times with 1 mL of iso-osmotic buffer, using a magnet for 5 minutes and discarding

the supernatant each time. After the last wash step, 1 mL of iso-osmotic buffer plus 1% BSA was added and the beads were incubated overnight at 4°C (tube B). Then beads (tube B) were washed twice and the contents of both tubes (A and B) were mixed and incubated for 1 hour at 4°C. The magnetic beads were pelleted as before and the supernatant discarded, followed by 5 washings with 1 mL of iso-osmotic buffer. For western-blot analysis, the material attached to the beads was resuspended in 60 µL of loading buffer and boiled for 5 minutes.

Transmission Electron Microscopy

The sEV-enriched pellet was fixed with 2% paraformaldehyde, placed on Formvar-carbon-coated grids, and observed using electron microscopy (Thery et al., 2006). The mean sizes were obtained from n > 50 vesicles from at least 2 independent sEV preparations per experimental group.

Nanoparticle Tracking Analysis

The size distribution and concentration of the sEVs were analyzed with the NanoSight LM-10 equipment (Malvern Instruments) and using a green laser. sEVs were diluted 1:100 with PBS. Three videos, each 60 seconds long, were recorded per sample using a detection threshold of 10 (NTA 3.1Software) for comparison.

High-Resolution Proteomic Analysis

sEV proteins were separated using polyacrylamide gradient gel electrophoresis. Each lane was divided into 8 sections to perform in-gel digestion according to Kolodziej et al., 2016.

Liquid chromatography followed by tandem-mass spectrometry (MS/MS) of the sample fractions was performed on a hybrid dual-pressure linear ion trap/orbitrap mass spectrometer (LTQ Orbitrap Velos Pro, Thermo Scientific) equipped with an EASY-nLC Ultra HPLC (Thermo Scientific). Peptide samples were dissolved in 10 µL of 2% acetonitrile/0.1% trifluoric acid and fractionated on a 75-µm i.d., 25-cm PepMap C18-column, packed with 2 µm of resin (Dionex, Germany). Separation was achieved by applying a gradient of 2% to 35% acetonitrile in 0.1% formic acid over 150 minutes at a flow rate of 300 nL/min.

The LTQ Orbitrap Velos Pro MS was exclusively used for CID-fragmentation when acquiring MS/MS spectra, which consisted of an orbitrap full mass spectrometry (MS) scan followed by up to 15 LTQ MS/MS experiments (TOP15) on the most abundant ions detected in the full MS scan. The essential MS settings were as follows: full MS (resolution, 60,000; mass to charge ratio range, 400–2000); MS/MS (Linear Trap; minimum signal threshold, 500; isolation width, 2 Da; dynamic exclusion time setting, 30 seconds; and singly charged ions were excluded from the selection). Normalized collision energy was set to 35%, and activation time was set to 10 milliseconds.

Raw data processing and protein identification were performed by ProteomeDiscoverer 1.4 (Thermo Scientific) and a combined database search used the Sequest and Mascot algorithms. The false discovery rate was calculated by the Percolator 2.04 algorithm and was set to < 1%. An Ingenuity Pathway Analysis was used for network analysis of functional interactions of proteins.

The MS proteomics data obtained in this study have been deposited to the ProteomeXchange Consortium via the PRIDE partner repository with the dataset identifier PXD009085 (Vizcaino et al., 2016). The ProteomeXchange dataset has been

made public via the PRIDE database, with the following details: ProteomeXchange title: rat serum exosomes after restriction stress, ProteomeXchange accession: PXD009085, PubMed ID: Not applicable, Publication DOI: Not applicable, Project Webpage: http://www.ebi.ac.uk/pride/archive/projects/PXD009085, FTP Download: ftp://ftp.pride.ebi.ac.uk/pride/data/archive/2018/12/PXD009085.

Materials and Antibodies

Reagents were acquired in Sigma-Aldrich (Santiago, Chile) unless otherwise specified. Primary antibodies were used at dilutions of 1:1000 against MAP2 (MAB378, Merck Millipore); TSG101 (Ab83, Abcam); Flotillin-1 (610821, BD Transduction Laboratories); CD63 (sc-15363, Santa Cruz Biotechnology); GM130 (Ab1299, Abcam); GFAP (Mab C 2032-28B, US Biological); GFP (Ab6673, Abcam); GFP (MAB3580, Merck Millipore); EAAT2 (AGC022, Alomone, Israel); SUMO 1 (Ab32058, Abcam); SUMO 2/3 (Ab109005, Abcam), and aldolase C (sc12065, Santa Cruz Biotechnology). In addition, Dr Richard Hawkes (University of Calgary, Alberta, Canada) kindly provided a monoclonal antibody against aldolase C, which in western blots recognizes a polypeptide antigen of 36 kD tested across species, including mammals (Sillitoe et al., 2005). Secondary antibodies Alexa Fluor 488 Donkey Anti-Goat IgG (# A11055) and Alexa FluorR 555 Donkey Anti-Mouse IgG (# A28180) coupled to fluorescent probes were purchased from Invitrogen (Thermo Fisher Scientific).

Statistical Analysis

The data are presented as the mean±SEM. Semiquantitative analysis of western blots was evaluated by comparing the relative optic densities of bands (fold change of stress over no stress) after restraint and immobilization using the Mann-Whitney test. In turn, the significant differences in each dataset, with a hypothetical value of 1 (no change), were assessed with a Wilcoxon-signed rank test. Statistical significance was set at $P < .05$ (*, #) or $P < .01$ (**, ##).

Results

To identify peripheral markers in sEVs, rats were exposed to no stress or to stress by restraint or by immobilization for 10 days (Figure 1A). The stress protocol induced similar depressive-like behaviors that were reverted by either fluoxetine (after restraint) or reboxetine (after immobilization) (Ampuero et al., 2015). In addition, different body weight gain and sucrose preferences were observed among experimental groups (Supplementary Figure 1a–b). To investigate whether these differences could be reflected in blood biomarkers, serum sEVs were isolated by ultracentrifugation, and the $100\,000 \times g$ pellet was used in the present study. The obtained material was characterized by size, concentration, and the presence of proteins known to be exosome markers (Figure 1). Using transmission electron microscopy, morphological characteristics of EVs were observed (Figure 1B). The mean diameters of the vesicles obtained from animals exposed to no stress, restraint, or immobilization were 58.3±2.9, 53.7±2.7, and 49.7±2.3 nm, respectively (n > 50 vesicles obtained from at least 2 independent EV preparations per experimental group) (not shown). As expected, when the size distribution was assessed by nanoparticle tracking analysis (NTA), larger mean sizes were obtained after fitting Gaussian distributions to the data (139.7±37.9, 140.7±35.9, and 140±35.3 nm, respectively) (Figure 1C). In these NTA profiles, major peaks of abundant

vesicles were observed at 125 (no stress), 135 (restraint), and 115 (immobilization) nm (n=4–6 independent EV preparations per experimental group). The larger sizes observed with the NTA are consistent with the literature and the fact that several factors contribute to size shifts, for example, NTA detects the diameter of vesicles in solution based on their Brownian motion, while clusters of particles, most likely cross-linked by proteins such as tetherin, contribute to the measures (Sokolova et al., 2011; Edgar et al., 2016). Thus, it can be concluded that the sizes of the isolated vesicles are compatible with sEVs, such as exosomes, and that these are highly comparable between the experimental conditions investigated.

We finally performed a biochemical characterization of these sEVs. Equal amounts of total protein per lane were used for the western blots to detect the presence of proteins that are considered markers of exosomes (Figure 1E). Surprisingly, we observed quantitative variations in the selected marker proteins among the experimental groups (Figure 1E). In this way, while the abundance of tetraspanin CD-63 decreased after stress by restraint, it did not change after immobilization. After reprobing the same blots, the amount of flotillin was found to be higher in the sEVs after restraint than after immobilization, while the abundance of a member of the endosomal sorting complexes required for transport, TSG-101, increased after restraint but demonstrated no statistically significant changes after immobilization. These results suggested that the used vesicle fraction was heterogeneous with regard to the cell types that generate them in each case and/or that the molecular mechanisms involved in their biogenesis and cargo selection vary among experimental conditions. In this vein, the variability of putative sEV markers has been recently discussed (Kowal et al., 2016). To decipher brain-derived proteins that might vary significantly in serum sEVs of repetitively stressed rats, high-resolution MS-based proteomic analysis was performed.

Proteome of EVs After Stress

We postulated that the EVs proteome might serve as a systemic biomarker of stress or of different stress protocols associated with depressive-like behaviors. In total, 929 proteins were detected across the 3 experimental conditions (Figure 2). Interestingly, 128 proteins were detected exclusively under no stress, while 187 and 181 were selectively detected after restraint or immobilization, respectively. Database-assisted accession of the potential tissue where the proteins originate from, detected in the respective proteomes, revealed that after stress by restraint, the proteins expressed in the brain increased from <25% to >35% (Figure 2B). Since proteins that are expressed in astrocytes can be detected in the CSF (Sandoval et al., 2013), we overlaid a Venn diagram with the proteome data from the astrocyte-derived EVs. This Venn analysis revealed that a proportion of the proteins present in serum sEVs is also present in sEVs isolated from the conditioned medium of astrocytic cultures (Figure 2C).

To further analyze the proteomic data, we focused on proteins that were unique in only one of the experimental conditions and performed an Ingenuity Pathway Analysis in which we imposed an upper limit of 35 proteins per pathway. Here, we showed only the main pathways given by the analysis, that is, the networks containing the highest number of proteins detected per condition (Figure 3A–C). In the case of no stress, the pathway points to cellular protection and to intracellular trafficking/exosome biogenesis and secretion. Notably, this pathway contains as many as 25 identified proteins (gray
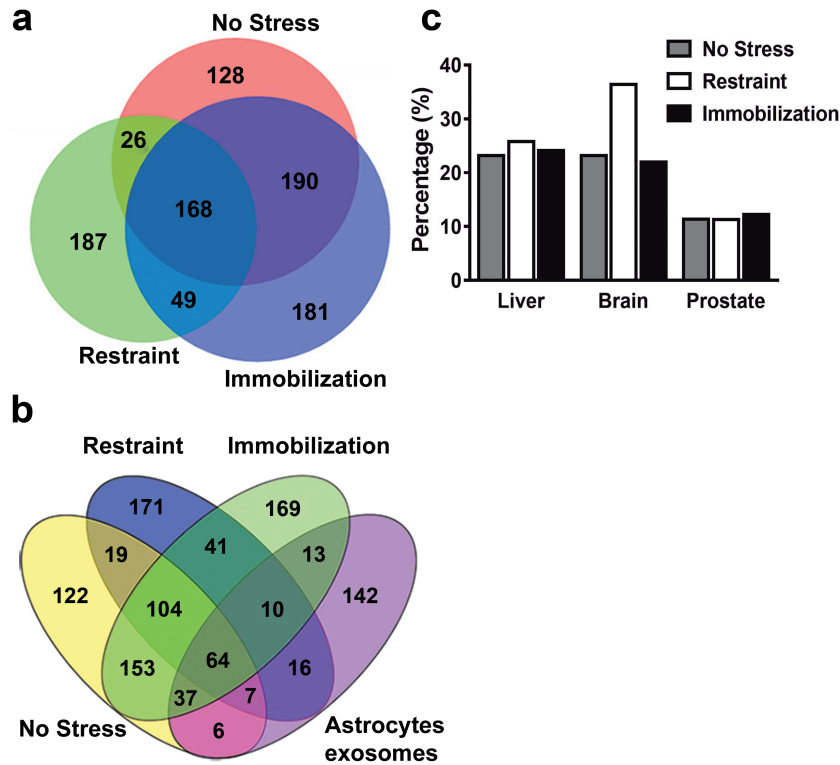
Figure 2. Proteomic analysis of extracellular vesicles (EVs) show that after restraint, proteins that are expressed in the brain are increased. (a) Venn analysis of the identified proteins in the experimental conditions. (b) Venn analysis of the identified proteins including the proteome of astrocyte small extracellular vesicles (sEVs). (c) The percentage of expression of the identified proteins in different body organs is shown (obtained with DAVID Bioinformatics Resources 6.8 [NIAID, NIH]).

symbols). In contrast, in the case of restraint, proteins more abundantly related to one cellular pathway indicate cellular stress (22 proteins), including proteins of the 26 S proteasome and others that are known EV components, such as heat shock proteins. The presence of C1QTNF5 and hexokinase 1 suggest mitochondrial dysfunction is a phenomenon associated with psychiatric disorders (Park et al., 2009; Regenold et al., 2012; Glombik et al., 2017), a point that will be further addressed in the discussion. In turn, in the case of immobilization, the main pathway also pointed to cellular stress pathways (27 identified proteins), including components of the 20 S proteasome and proinflammatory pathways converging on the transcription factor NF-κB, which is in turn a known mediator of stress-induced inflammation and depressive behavior (Koo et al., 2010; Caviedes et al., 2017). Interestingly, the glucocorticoid binding protein SERPIN6A, involved in the delivery of glucocorticoids to sites of inflammation, was also detected. In addition, networks and the proteomic content of each experimental condition were compared with the proteins of astrocyte EVs (Figure 4A–D). Interestingly, the functional interpretation of these networks suggested that they are involved in disease processes, such as in neurological and psychological disorders (after restraint) and in neurological disorders and inflammatory responses (after immobilization).

On the other hand, common proteins found in restraint and immobilization and their absence in sEVs of nonstressed animals are possibly related to the expression of stress-related, depressive-like behaviors. Only 49 proteins were present in this category, which are related to transmembrane transport, synaptic transmission and plasticity, and regulation of the intracellular redox status. Moreover, several of them participate in cellular stress responses (e.g., apolipoprotein B, caspase-5,

ceruloplasmin, Myc target 1) and might serve as general stress indicators.

To further verify the presence of astrocytic proteins in serum sEVs, we investigated one of the previously described candidate proteins, aldolase C, by using western-blot analysis (Figure 5). As shown in Figure 5A–B, a notable increase in the level of this protein was observed after restraint, while the opposite occurred after immobilization. In line with this, a typical astrocytic forebrain protein, GFAP, was also present in the sEVs and revealed similar changes. Other protein levels were not altered among the experimental conditions, such as β-tubulin, actin, and caveolin 1 (Supplementary Figure 2a), while 2 brain proteins that were found in the proteome, reelin and synaptophysin, decreased or changed differentially under each stress condition, respectively. Thus, while some proteins showed selective enrichment after restraint, others changed in the same direction under both stress conditions and a different subset did not change.

Surprisingly, aldolase C and synaptophysin were found to have higher molecular weights than expected (Figure 5A). To explain this discrepancy, we hypothesized that part of the sEV protein cargo undergoes posttranslational modifications that are responsible for decreased electrophoretic mobility. We focused on aldolase C, and to confirm the identity of this protein, we used 4 different antibodies generated against different antigenic zones of the protein (Figure 5C) in addition to a monoclonal antibody kindly provided by Dr. Richard Hawkes. All of them detected a protein with a molecular weight that was increased by approximately 20 kDa, confirming that a modified protein is present in sEVs (Figure 5D). In silico analysis revealed that aldolase C contains SUMO-interacting motifs as well as canonical sequences and lysine residues that are predicted to undergo SUMOylation (shown in the upper panel of Figure 5E).

Figure 3. Network analysis of proteins identified exclusively in one of the experimental conditions (no stress, restraint, or immobilization). Dotted lines indicate indirect interactions; solid lines represent direct interactions between proteins. (a) Network analysis of the proteins identified uniquely in the small extracellular vesicles (sEVs) of the no stress group indicated the convergence of survival pathways/cell protection and intracellular trafficking. ABCB8, ATP-binding cassette, subfamily B (MDR/TAP), member 8; aconitase, aconitate hydratase; actin, G-actin; Akt, AKT1/2/3; AP1B1, adaptor protein complex AP-1, β 1 subunit; ARF1, ADP-ribosylation factor 1; CLTA, clathrin, light chain A; DBNL, drebrin-like protein; DNM3, dynamin 3; dynamin, dynamin GTPase; FYB, FYN binding protein; NUCB2, nucleobindin 2; PARK7, parkinson protein 7; PBXIP1, pre-B-cell leukemia transcription factor interacting protein 1; RPS20, ribosomal protein S20; SCAMP1, secretory carrier membrane protein 1; SKAP2, src kinase associated phosphoprotein 2; SLC2A4, solute carrier family 2 (facilitated glucose transporter), member 4; SMPD3, sphingomyelin phosphodiesterase 3; SNAP23, synaptosomal-associated protein 23; STX4, syntaxin 4; STXBP2, syntaxin binding protein 2; Tpm1, tropomyosin 1α; Tpm2, tropomyosin 2β; Tpm3, tropomyosin 3; VAMP7, vesicle-associated membrane protein 7; ZYX, zyxin. (b) Network analysis of proteins identified uniquely in the sEVs after restraint indicated proteins

Moreover, SUMOylation acts as a sorting factor for targeting proteins to sEVs (Kunadt et al., 2015). To test whether aldolase C in sEVs was SUMOylated, we first performed western-blot analyses to detect SUMO 1 and SUMO 2/3 in sEVs (Figure 5F). Interestingly, a SUMO 2/3 band coincided with aldolase C, while SUMO 1 presented bands of lower molecular weight as well as a minor band at the molecular weight detected by the aldolase C antibodies. We therefore immunoprecipitated aldolase C and SUMO 1 from sEVs. We found that the aldolase C and SUMO immunoprecipitates were positive for SUMO (upper western blot of Figure 5G) and for aldolase C (lower western blot), strongly suggesting that the protein detected by the aldolase C antibodies contained this posttranslational modification. We finally examined whether blood sEVs carry recombinant aldolase C-GFP when the protein is exclusively expressed in the brain.

Aldolase C in the Serum sEVs Is Derived From the Forebrain

To determine whether aldolase C in serum EVs originates from brain astrocytes, we transferred aldolase C-GFP or GFP to astrocyte progenitors at embryonic days 18 to 19, positioning the positive electrode on a frontal position. The electroporated rats grew for 2.5 to 3 months (Figure 6A). Blood was collected, and the brains were prepared for immunofluorescence against GFP and GFAP as a marker of astrocytes. Under the experimental conditions used, aldolase C-GFP-positive and GFAP-positive cells were mainly detected in proximity to the lateral ventricles and in the hippocampus (Figure 6B–C). In addition, transduced astrocytes were detected in the cerebral cortex (Supplementary Figure 2b), and astrocytic processes surrounding the blood vessels, which were compatible with astrocytic end feet, were observed (data not shown). The nonelectroporated hemisphere did not stain for GFP, and the subcortical nuclei were also negative for electroporated cells. The cerebral cortex contained a lower colocalization of GFAP and GFP (Supplementary Figure 1b, middle), while in a few cases, single GFP-stained cells resembling neurons were observed (Supplementary Figure S1b, top). We did not go further into this observation and cannot differentiate whether the detected cell was an electroporated neuron or whether it was a neuron that had taken up massive amounts of aldolase C. To assess whether aldolase C-GFP, when expressed in brain cells, could be detected in serum sEVs, we performed western blots of these sEVs. We found that the recombinant protein aldolase C-GFP was detected using an aldolase C antibody (left) or the GFP antibody (right) (Figure 6D), revealing bands of approximately 70 kDa both with the GFP antibody, whereas with the anti-aldolase antibody, both the recombinant as well as the endogenous proteins were detected. Note that astrocyte

homogenates contain 2 protein bands corresponding mainly to the expected molecular weight form of aldolase C (approximately 36 kDa), while the higher molecular weight form (possibly SUMOylated) was also weakly detectable in this homogenate. Interestingly, sEVs contained only the endogenous high-molecular-weight form of aldolase C-GFP. As a control, animals were electroporated with GFP (Figure 6E), and similarly, serum EVs were obtained. In the left blot, the expected aldolase C forms were detected, whereas GFP could not be detected in the sEV fractions, suggesting that aldolase C is actively targeted to sEVs and that the contribution of GFP to this process is negligible.

Using a different experimental strategy to enrich astrocyte-derived EVs, we immune-isolated sEVs carrying the glial glutamate transporter EAAT2 (Figure 6F). The precipitate (i.e., EAAT2-positive vesicles) contained aldolase C, and the protein was highly enriched with respect to the input, in which aldolase C could be detected only after overexposure of the membrane (right lanes). Note that aldolase C was weakly detected in the control IgG. This is a common phenomenon attributed to the presence of sumo-interacting motifs in IgGs. Thus, we assured that the control IgG was added at similar or even higher amounts than the anti-aldolase antibody (last row). Taken together, our results showed that aldolase C, expressed in astrocytes, can be collected in serum sEVs and could therefore constitute a potential stress biomarker.

Discussion

In this work, we showed that blood sEVs contain proteins that are expressed in brain cells, revealing a direct communication between brain glial cells and the rest of the body. In addition, we demonstrated a different content of sEV proteins in 2 animal stress models showing depressive-like behaviors that responded selectively to antidepressant treatments (Ampuero et al., 2015). Thus, this work has notable projections in the field of biomarker research in humans, intended to distinguish among psychiatric diseases or subtypes of mood disorders but also on common biomarkers of depressive-like behaviors. On the other hand, the presence of brain-derived sEVs in the blood suggested that they might target some peripheral organs/tissues with some preference, participating in this way in brain-to-periphery signaling. While the increased presence of aldolase C in EAAT2-affinity isolated EVs supports the notion that astrocyte EVs are contributing to the differential proteome, it remains unknown to what extent other brain cells participate as peripheral EVs donors. In this way, neurons and microglia might be additional cellular sources, as suggested by the presence of synaptophysin, reelin, or calcium and calmodulin-dependent kinase II (mainly expressed in neurons), just to name a few. Similarly, many other

related to cellular stress responses. 26 s Proteasome, Proteasome; BAHCC1, BAH domain and coiled-coil containing 1; C1QTNF5, C1q and tumor necrosis factor related protein 5; CEP250, centrosomal protein 2; CHD8, chromodomain helicase DNA binding protein 8; CLIC1, chloride intracellular channel 1; ERK, p42/44 MAPK; HECTD1, HECT domain-containing E3 ubiquitin protein ligase 1; Histone h3, Histone H3B; HK1, hexokinase 1; Hsp90, Heat shock protein 90 kDa; HSPA2, heat shock 70 kDa protein 2; HSPA8, Heat shock 70kD Protein 8; IDH1, isocitrate dehydrogenase 1; KHSRP, KH-type splicing regulatory protein; MAP1B, microtubule-associated protein 1B; MAPT, microtubule-associated protein tau; MTMR1, Myotubularin Related Protein 1; NCL, nucleolin; NOA1, nitric oxide associated 1; POLR1A, polymerase (RNA) I polypeptide A; Rnr, 47S Pre-rRNA, Ribosomal; RPS23, ribosomal protein S23; SPAG9, sperm associated antigen 9; SYPL2, synaptophysin-like 2; TNRC6A, trinucleotide repeat containing 6A; TUFM, Tu translation elongation factor. (c) Network analysis of the proteins identified uniquely in the sEVs after immobilization paradigm indicated protein components related to cancer and hematological and immunological diseases. 20 S proteasome, 20 S Core Complex; ABCC1, ATP-binding cassette, subfamily C (CFTR/MRP); CCT3:, chaperonin-containing TCP1, subunit 3 (gamma); CLIP2, CAP-GLY domain-containing linker protein 2; elastase, serine elastase; OC100360846/Psmb6, proteasome subunit β 6; MYH14, myosin, heavy chain 14; MYH7, beta cardiac myosin heavy chain; MYH8, myosin, heavy chain 8; NFkB (complex), transcription factor nuclear factor κ b; PGRMC1, progesterone receptor membrane component 1; PRKCB, protein kinase C β II; PSMA3, proteasome subunit α 3; PSMA5, proteasome subunit α 5; PSMA6, proteasome subunit α 6; PSMB1, proteasome subunit β 1; PSMB3, proteasome subunit β 3; PSMB4, proteasome subunit β 3; PSMB5, poteasome subunit β 5; PSMB7, proteasome subunit β 7; PSME1, Proteasome activator pa28 α subunit; SERPINA6, Corticosteroid-binding globulin, serine (or cysteine) peptidase inhibitor; SERPINB10, serine (or cysteine) peptidase inhibitor, clade B; SERPINB6, serine (or cysteine) peptidase inhibitor, clade B, member 6; TUBB2A, tubulin, β 2A; TUBB4B, tubulin, β 4B; TUBB6, tubulin, β 6.
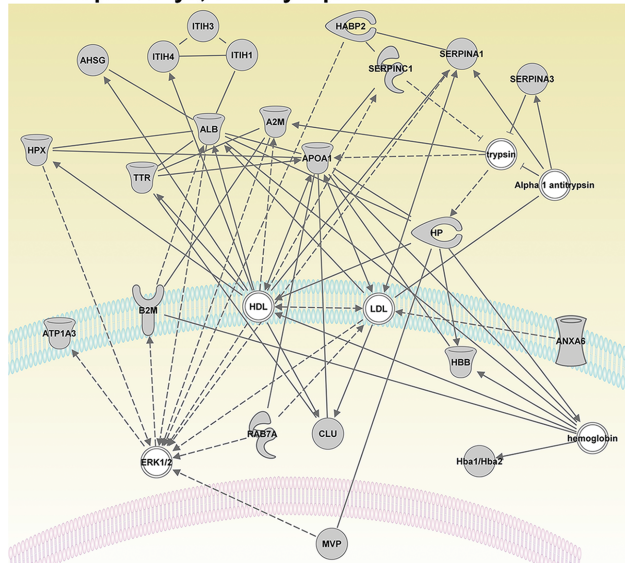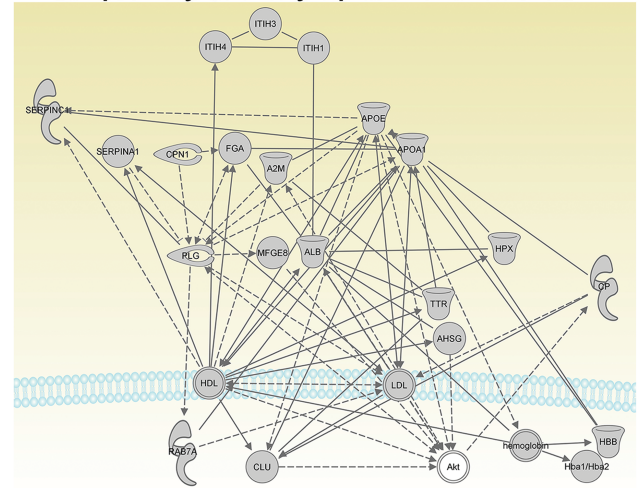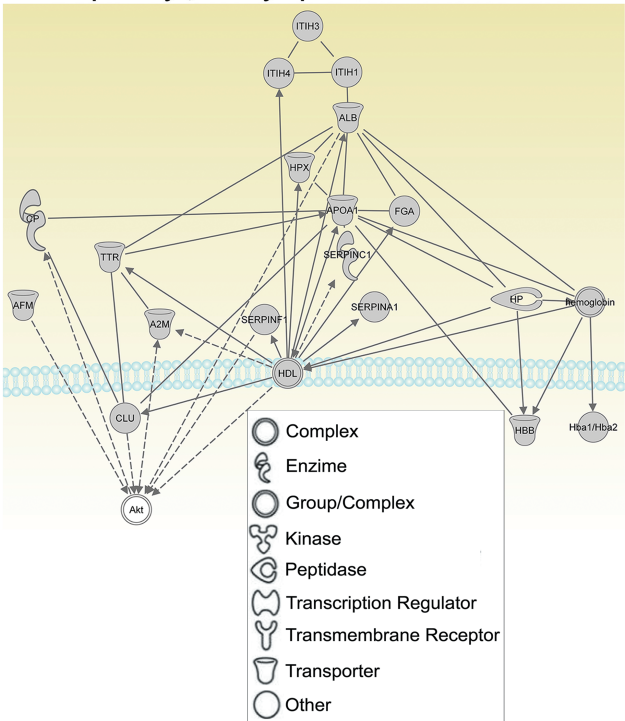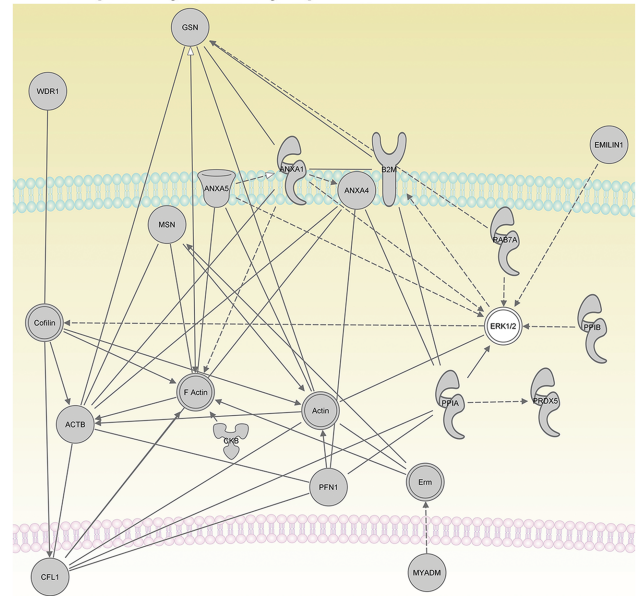
Figure 4. Network analysis of proteins in serum small extracellular vesicles (sEVs) and in astrocyte sEVs. Dotted lines indicate indirect interactions; solid lines represent direct interaction between proteins. (a) Network analysis of proteins obtained from serum sEVs of no stress group also present in astrocytes sEVs indicated protein components related to metabolic disease, endocrine system disorders, and gastrointestinal disease. A2 M, Alpha-2-microglobulin; AHSG, alpha-2-HS-GLYCOPROTEIN; ALB, Albumin 1; Alpha 1 antitrypsin, Alpha 1 antitrypsin; ANXA6, Annexin VI; APOA1, apolipoprotein A-I; ATP1A3, Na+/K+ ATPase alpha3; B2 M, beta-2-MICROGLOBU-LIN; CLU, clusterin; ERK1/2, p42/44 MAPK; HABP2, hyaluronic acid binding protein 2; Hba1/Hba2, hemoglobin, α 1, hemoglobin, α 2; HBB, Beta-globin; HDL, high-density lipoprotein; HP, haptoglobin; HPX, hemopexin; ITIH1, inter-alpha trypsin inhibitor, heavy chain 1; ITIH3, inter-alpha trypsin inhibitor, heavy chain 3; ITIH4, inter-alpha trypsin inhibitor, heavy chain 4; LDL, low-density lipoprotein; MVP, major vault protein; RAB7A, member RAS oncogene family, RAB7A; SERPINA1, serine (or cysteine) peptidase inhibitor, clade A; SERPINA3, serine (or cysteine) peptidase inhibitor, clade A, member 3 M; SERPINC1, serine (or cysteine) peptidase inhibitor, clade C, member 1; TTR, Transthyretin isomer 1. (b) Network analysis of the proteins obtained from serum sEVs after restraint also present in astrocytic sEVs indicating the protein components related to metabolic disease, neurological disease, and psychological disorders. A2 M, alpha-2-macroglobulin; AHSG, alpha-2-HS-GLYCOPROTEIN; Akt, AKT1/2/3; ALB, Albumin 1; APOA1, apolipoprotein A-I; APOE, Apolipoprotein E; CLU, clusterin; CP, ceruloplasmin; CPN1, carboxypeptidase N; FGA, Fibrinogen A α; Hba1/Hba2, hemoglobin, α 1, hemoglobin, α 2; HBB, Beta-globin; HDL, high-density lipoprotein; HPX, hemopexin; ITIH1, inter-alpha trypsin inhibitor, heavy chain 1; ITIH3, inter-alpha trypsin inhibitor, heavy chain 3; ITIH4, inter-alpha trypsin inhibitor, heavy chain 4; LDL, low-density lipoprotein; MFGE8, milk fat globule-EGF factor 8 protein; PLG, plasminogen; RAB7A, member RAS oncogene family, RAB7A; SERPINA1, serine (or cysteine) peptidase inhibitor, clade A; SERPINC1, serine (or cysteine) peptidase inhibitor, clade C, member 1; TTR, Transthyretin isomer 1. (c) Network analysis of the proteins obtained from the serum sEVs after immobilization paradigm

tissues and cell types outside the CNS release EVs: for example, cells of the immune system are a prominent source of blood EVs in health and disease (Ventimiglia and Alonso, 2016). Here, we show that the impact of stress on the brain is reflected by a differential proteome of sEVs that can originate in brain cells.

The biological actions of brain-derived sEVs in peripheral organs have, until now, been unexplored in areas such as comorbidity among stress-induced disorders. Brain-to-periphery communication mediated by sEVs has been documented in animal models of inflammation: in such a way, endothelial cell-derived EVs transfer tight junction proteins to peripheral blood leukocytes in experimental autoimmune encephalomyelitis (Paul et al., 2016) and mediate the inflammatory hepatic acute-phase response that is triggered following focal inflammation of the brain parenchyma (Couch et al., 2017). Circulating EVs also increase after traumatic brain injury and, when obtained in vitro under proinflammatory conditions (from macrophages or endothelial cell lines), they regulate the inflammatory response both in the periphery and CNS (Hazelton et al., 2018). A distant negative effect in the lungs, the bystander effect, was proposed to be mediated by astrocyte-derived EVs after focal ionizing radiation of the brain (Cai et al., 2017b). In the latter case, although the route of communication remains unknown, EVs isolated from cultured astrocytes could recapitulate the bystander effect. Moreover, after a focal brain inflammation in the striatum, astrocyte-derived EVs regulate the distant acute liver response and trigger the transmigration of leukocytes into the brain parenchyma (Dickens et al., 2017). Taken together, these studies support the notion that brain-derived EVs can reach peripheral blood and organs, and we have added in vivo evidence that specific stress conditions modify the molecular cargo of sEVs.

The search for biological markers of subtypes of mood disorders, their severity, and differential drug responsiveness has attracted increasing levels of interest (Lv et al., 2016). Proposed biomarkers include neuroimaging biomarkers, such as those for functional magnetic resonance imaging (Lener and Iosifescu, 2015; Drysdale et al., 2017), genomic markers (Licinio et al., 2009; Lin et al., 2014) or levels of molecules in the blood, such as proteins (i.e., cytokines, neurotrophins, and/or their receptors), mRNAs, or miRNAs (Cattaneo et al., 2016; Maffioletti et al., 2016; Siwek et al., 2017). In our study, several proteins detected in sEVs after both restraint and immobilization have already been proposed as markers of depressive disorders or of their symptoms, such as thioredoxin, a redox protein that protects against oxidative stress (Aydin et al., 2018), or the voltage-dependent anion selective ion channels that regulate mitochondrial cytochrome c release (Glombik et al., 2015). A large proportion of the differential proteome identified here participates in the regulation of mitochondrial function and oxidative stress, supporting the implication of energy metabolism changes (especially oxidative phosphorylation and glycolysis) in stress-associated disorders (Corena-McLeod et al., 2013; Detka et al., 2015). Thus, the proteome of blood sEVs reflects in part molecular neurobiological processes activated by repetitive stress (Krishnan and Nestler,

2010; Carboni, 2015). Interestingly, the rapid-acting antidepressant effect of ketamine is mediated by the regulation of mitochondrial function in the hippocampus (Weckmann et al., 2017). Similarly, fluoxetine (but not imipramine) upregulates proteins, for example, Aldolase A and Park7, involved in mitochondrial biogenesis and oxidative defense in the hippocampus (Glombik et al., 2017), and these protective molecules were not detected after stress in EVs. Other mitochondrial antioxidant proteins, such as Superoxide Dismutase and Cytochrome c oxidase subunits, were found in no stress or in no stress and immobilization, respectively, suggesting differences in the redox balance in the brain cells originating EVs among stress subtypes. In accordance, paroxetine, a selective serotonin reuptake inhibitor, restored Superoxide Dismutase 2 (and voltage-dependent anion selective ion channel) levels along with reverting depressive behavior in mice (Whittle et al., 2011). Finally, increased GFAP expression probaby reveals glial activation, which has been recognized as a putative marker of suicidal behavior (Torres-Platas et al., 2016).

The mass spectrometric approach carried out in this work identifies the proteome of serum sEVs in a qualitative manner. Nevertheless, even if the identification of a protein is reliable and proven by false discovery rate calculations (set to <1%), the condition-dependent comparison of low abundant proteins in sEVs might result in a blurred line between detection and missed identification. Surprisingly, the selective Venn analysis of the very highly abundant proteins of each experimental condition (identified by more than 10 different tryptic peptides) revealed a similar outcome to comparing all of the identifications: while only 20 (18%) remained unique to the control condition (no stress), 59 (37%) were unique to the immobilized group, and 49 (50%) were unique to the restraint group. This supported the assumption that the described differences in EVs protein content reflect a biological phenomenon rather than a proteomic analytical artifact. When we assigned the proteins to gene ontology terms and compared them to random protein lists matched in size as described in Kahne et al., 2016, the most prominent upregulation was found for the term "C: extracellular exosome," supporting the sufficient quality of used sEV preparations.

With the present experimental strategy that was used to transfer aldolase C-GFP to forebrain astrocytes, using the GFAP promoter in the helper plasmid, we cannot rule out that a proportion of the recombinant protein in serum sEVs was derived from other cell types in addition to astrocytes. Consistent with low neuronal precursor proliferation at the age of electroporation (i.e., impeding the integration of the plasmid into the genome and, thus, its stable expression), we observed very few neurons when examining the brain slices. In contrast, ependymal cells still proliferate at E18-E19, and our observations were consistent with the transfer of aldolase C-GFP to cells lining the ventricular walls (Bruni, 1998). However, until now there is no evidence in the literature that ependymal cells are altered in psychiatric diseases or that they could secrete sEVs with differential molecular cargo (Comte et al., 2012).

---

also present in astrocytic sEVs. Network related to neurological and metabolic diseases. A2 M, alpha-2-macroglobulin; AFM, serum albumin, α-Alb; Akt, AKT1/2/3; ALB, albumin 1; APOA1, apolipoprotein A-I; CLU, clusterin; CP, ceruloplasmin; FGA, alpha-fibrinogen; Hba1/Hba2, hemoglobin, α 1, hemoglobin, α 2; HBB, Beta-globin; HDL, high-density lipoprotein; hemoglobin, hemoglobin; HP, haptoglobin; HPX, hemopexin; ITIH1, inter-alpha trypsin inhibitor, heavy chain 1; ITIH3, inter-alpha trypsin inhibitor, heavy chain 3; ITIH4, inter-alpha trypsin inhibitor, heavy chain 4; SERPINA1, serine (or cysteine) peptidase inhibitor, clade A, member 1; SERPINC1, serine (or cysteine) peptidase inhibitor, clade C; SERPINF1, serine (or cysteine) peptidase inhibitor, clade F, member 1; TTR, transthyretin isomer 1. (d) Network related to inflammatory response. ACTB, actin β; Actin, G-actin; ANXA1, annexin A1; ANXA4, annexin A4; ANXA5, annexin A5; B2 M, beta-2-MICROGLOBULIN; CFL1, cofilin 1; CKB, Creatine kinase b chain; Cofilin; EMILIN1, elastin microfibril interfacer 1; ERK1/2, p42/44 MAPK; Erm; F Actin, Filamentous actin; GSN, Gelsolin; MSN, moesin; MYADM, myeloid-associated differentiation marker; PFN1, profilin 1; PPIA, peptidylprolyl isomerase A; PPIB, peptidylprolyl isomerase B; PRDX5, Peroxiredoxin 5; RAB7A, member RAS oncogene family, RAB7A; WDR1, WD repeat domain 1.
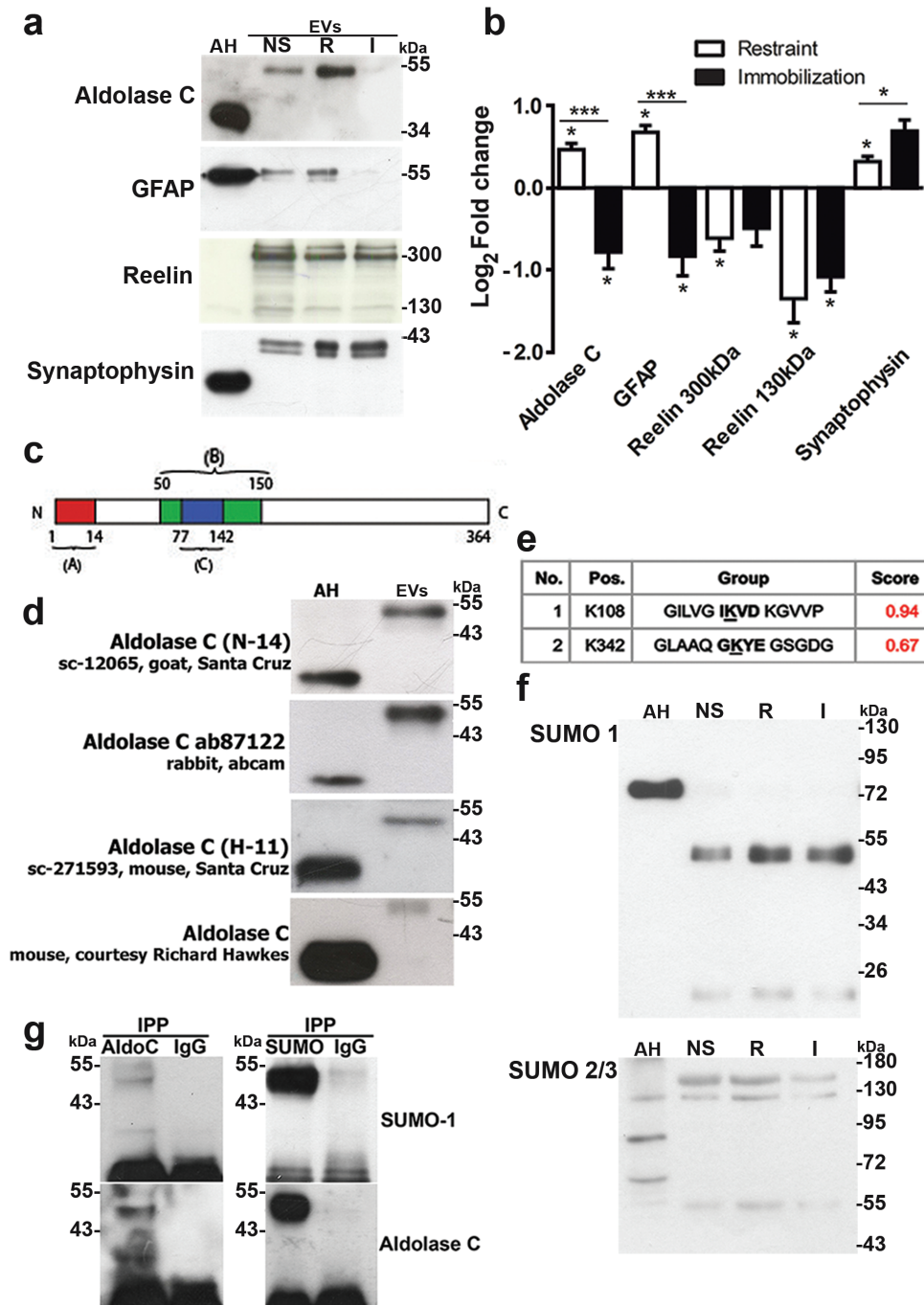
Figure 5. Proteins expressed in astrocytes (aldolase C and glial fibrillary acid protein [GFAP]) are differentially present in small extracellular vesicles (sEVs) obtained after restraint or immobilization. (a) Representative western blots of the indicated proteins and (b) corresponding densitometric quantification. (c) Representation of the antigenic peptides that were used for generation of the Santa Cruz antibodies (A and C), while B indicates the antigenic peptide that was used for the generation of the Abcam antibody. Finally, a monoclonal antibody generated against a crude homogenate of cerebellum and electrosensory lateral line lobe from a weakly electric fish was used (gift from Dr. Richard Hawkes, University of Calgary). (d) Western blots of aldolase C using antibodies of the different sources and directed against different antigenic peptides in the protein. (e) Possible small ubiquitin-like modifier (SUMO)ylating residues of aldolase C are indicated. (f) Western blots of sEVs using anti-SUMO antibodies. (g) Western blots of immunoprecipitated aldolase C (left) and SUMO (right) using SUMO antibody (upper) or aldolase C antibody (lower). The IgG lane indicates the respective control conditions. AH, astrocyte homogenates; I, stress by immobilization; NS, no stress; R, stress by restraint. N=5–7; #P<.05; ##P<.0 in Mann-Whitney tests (to compare pairs of data, i.e., restraint vs immobilization); *P<.05 in a Wilcoxon-signed rank test (to compare fold changes with a hypothetical value of 1 (no change).

It has already been proposed that proteins expressed in the brain constitute peripheral biomarkers of CNS diseases (Mustapic et al., 2017; Goetzl et al., 2018). Here, we provided direct evidence that blood EVs contain a recombinant protein that is exclusively expressed in brain cells, including astrocytes. With the electroporation strategy that was used, we mainly targeted astrocytes in the hippocampus and cells lining the lateral ventricles. The derived EVs could cross the blood-brain barrier
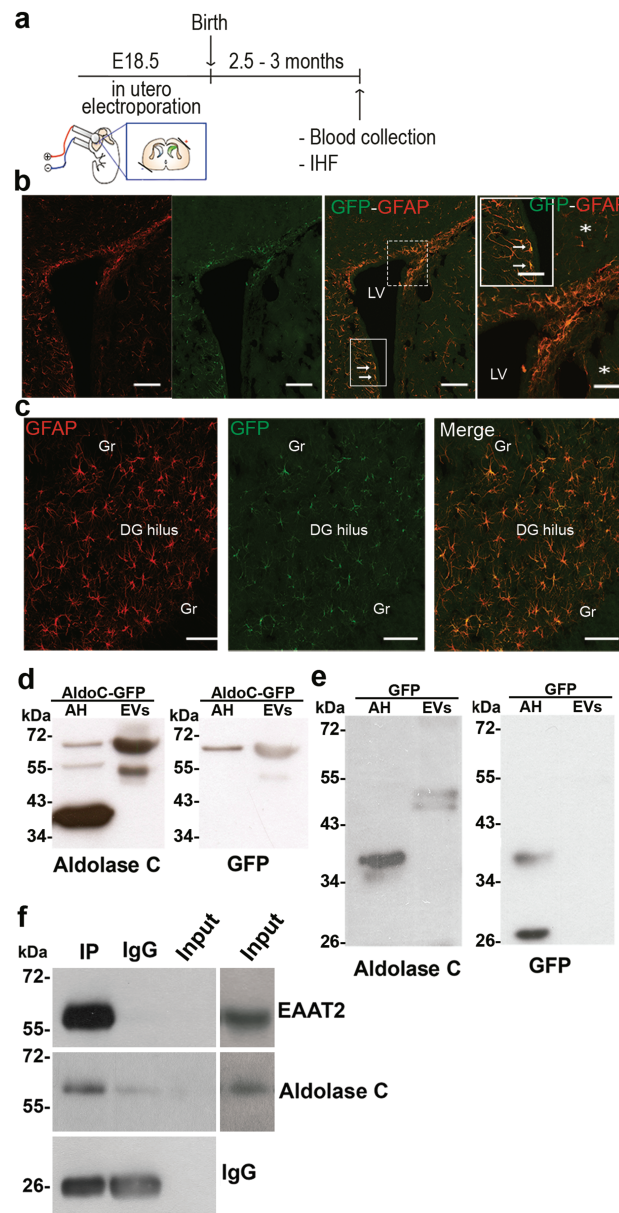
Figure 6. Aldolase C tagged with green fluorescent protein (C-GFP) expressed in forebrain astrocytes is detected in extracellular vesicles (EVs) isolated from the blood. (a) Scheme of the in utero electroporation. Forebrain astrocytes were transduced by in utero electroporation with aldolase C-GFP or GFP. Plasmids were injected into the left lateral ventricle on embryonic day 18.5. The orientation of the electrodes used to apply the voltage pulse is shown. (b) Immunohistofluorescent detection of glial fibrillary acid protein (GFAP) and GFP in coronal brain slices indicated that cells positive for both proteins were detected in the borders of the lateral ventricles (LV, indicated by arrows), and (c) in the hilus of the dentate gyrus (DG). Gr, granule cells. (d) Aldolase C (left) or GFP (right) was detected in astrocyte homogenates (AH) electroporated with aldolase C-GFP or in sEVs isolated from the serum of these animals. Note that in the sEVs, the modified form of aldolase C was detected (~ 55 kDa), as well as the recombinant protein (~ 70 kDa), which was also visible with the GFP antibody. (e) Aldolase C (left) or GFP (right) was detected in the astrocyte homogenates (AH) that were electroporated with GFP or in extracellular vesicles (sEVs) isolated from the serum of these animals. Note that in sEVs, the modified form of aldolase C was detected (~ 55 kDa), while in these animals, no GFP could be detected in the EVs. Observations were conducted in n = 5 independent animal groups (n = 4 rats per group for blood collection). (f) EVs bearing the glial glutamate transporter EAAT2 in their membrane are enriched in aldolase C. EVs were immunoisolated in nondenaturating conditions with an antibody directed against an extracellular epitope of EAAT2. The input lane was loaded with 8% of the EVs used for the precipitation procedure (i.e., 20 μg). Note that EAAT2 can only be detected in the input after overexposure of the same blot (right lanes), revealing a huge enrichment of EAAT2-bearing vesicles in the isolated material that in turn also contains higher aldolase C levels compared with the input EVs.

(BBB) by transcytosis, especially when considering the detected endfeet-like structures of electroporated astrocytes (Chen et al., 2016). In addition, the permeability of the BBB was altered after stress paradigms such as social defeat stress (Menard et al., 2017). Moreover, astrocyte-derived EVs were detected in the peripheral circulation under inflammatory conditions (Dickens et al., 2017; Willis et al., 2017). It still needs to be clarified whether the increased detection of astrocytic proteins in sEVs after restraint is a consequence of proinflammatory alterations in the BBB or a consequence of the increased sEVs release under certain stress conditions (Santha et al., 2015).

The shift in the molecular weight of aldolase C was compatible with its SUMOylation: SUMO peptides of 10 kDa produce band shifts of approximately 20 kDa because their

attachment creates a branch point in the protein chain explaining an additional retardation in-gel migration. Aldolase C contains a high number of lysine residues that could accept SUMO peptides as well as SUMO interacting motifs (Xue et al., 2006). Note that the detection of endogenously SUMOylated proteins has remained challenging because of the reversible and regulated nature of the process. Moreover, most of the SUMO substrates are not able to be detected by MS because after trypsinization, long peptides remain undigested. Thus, the fact that we did not identify aldolase C in our sEVs samples by MS but rather by western blot was also highly indicative of its presence in a SUMOylated form (Cai et al., 2017a). It is possible that synaptophysin, which was also detected with a higher molecular weight in blood EVs, belongs to the presynaptic protein pool that is regulated by SUMO (Girach et al., 2013; Matsuzaki et al., 2015). Overall, SUMOylation constitutes a novel form of protein cargo selection in EVs and may explain their higher apparent molecular weights (Villarroya-Beltri et al., 2014; Kunadt et al., 2015).

Taken together, our data provide evidence for a specific pattern of brain-derived protein cargo in serum sEVs after stress that might impact future studies aimed at understanding the pathogenesis and comorbidity of stress-related disorders.

Funding

Acknowledgments

Statement of Interest

None.

References

Akil H, Gordon J, Hen R, Javitch J, Mayberg H, McEwen B, Meaney MJ, Nestler EJ (2018) Treatment resistant depression: a multi-scale, systems biology approach. Neurosci Biobehav Rev 84:272–288.

Ampuero E, Luarte A, Santibañez M, Varas-Godoy M, Toledo J, Diaz-Veliz G, Cavada G, Rubio FJ, Wyneken U (2015) Two chronic stress models based on movement restriction in rats respond selectively to antidepressant drugs: aldolase C as a potential biomarker. Int J Neuropsychopharmacol 18:pyv038.

Aydın EP, Genç A, Dalkıran M, Uyar ET, Deniz İ, Özer ÖA, Karamustafalıoğlu KO (2018) Thioredoxin is not a marker for treatment-resistance depression but associated with cognitive function: an rTMS study. Prog Neuropsychopharmacol Biol Psychiatry 80:322–328.

Bruni JE (1998) Ependymal development, proliferation, and functions: a review. Microsc Res Tech 41:2–13.

Cai L, Tu J, Song L, Gao Z, Li K, Wang Y, Liu Y, Zhong F, Ge R, Qin J, Ding C, He F (2017a) Proteome-wide mapping of endogenous SUMOylation sites in mouse testis. Mol Cell Proteomics 16:717–727.

Cai S, Shi GS, Cheng HY, Zeng YN, Li G, Zhang M, Song M, Zhou PK, Tian Y, Cui FM, Chen Q (2017b) Exosomal mir-7 mediates bystander autophagy in lung after focal brain irradiation in mice. Int J Biol Sci 13:1287–1296.

Carboni L (2015) The contribution of proteomic studies in humans, animal models, and after antidepressant treatments to investigate the molecular neurobiology of major depression. Proteomics Clin Appl 9:889–898.

Cattaneo A, Ferrari C, Uher R, Bocchio-Chiavetto L, Riva MA, Consortium MRCI, Pariante CM (2016) Absolute measurements of macrophage migration inhibitory factor and interleukin-1-beta mRNA levels accurately predict treatment response in depressed patients. Int J Neuropsychopharmacol 19. doi: 10.1093/ijnp/pyw045.

Caviedes A, Lafourcade C, Soto C, Wyneken U (2017) BDNF/NF-κb signaling in the neurobiology of depression. Curr Pharm Des 23:3154–3163.

Colombo M, Raposo G, Théry C (2014) Biogenesis, secretion, and intercellular interactions of exosomes and other extracellular vesicles. Annu Rev Cell Dev Biol 30:255–289.

Comte I, Kotagiri P, Szele FG (2012) Regional differences in human ependymal and subventricular zone cytoarchitecture are unchanged in neuropsychiatric disease. Dev Neurosci 34:299–309.

Corena-McLeod M, Walss-Bass C, Oliveros A, Gordillo Villegas A, Ceballos C, Charlesworth CM, Madden B, Linser PJ, Van Ekeris L, Smith K, Richelson E (2013) New model of action for mood stabilizers: phosphoproteome from rat pre-frontal cortex synaptoneurosomal preparations. PLoS One 8:e52147.

Couch Y, Akbar N, Roodselaar J, Evans MC, Gardiner C, Sargent I, Romero IA, Bristow A, Buchan AM, Haughey N, Anthony DC (2017) Circulating endothelial cell-derived extracellular vesicles mediate the acute phase response and sickness behaviour associated with CNS inflammation. Sci Rep 7:9574.

Chen CC, Liu L, Ma F, Wong CW, Guo XE, Chacko JV, Farhoodi HP, Zhang SX, Zimak J, Ségaliny A, Riazifar M, Pham V, Digman MA, Pone EJ, Zhao W (2016) Elucidation of exosome migration across the blood-brain barrier model in vitro. Cell Mol Bioeng 9:509–529.

Chen F, LoTurco J (2012) A method for stable transgenesis of radial glia lineage in rat neocortex by piggybac mediated transposition. J Neurosci Methods 207:172–180.

Darcet F, Gardier AM, Gaillard R, David DJ, Guilloux JP (2016) Cognitive dysfunction in major depressive disorder. A translational review in animal models of the disease. Pharmaceuticals (Basel) 9. doi: 10.3390/ph9010009.

Detka J, Kurek A, Kucharczyk M, Głombik K, Basta-Kaim A, Kubera M, Lasoń W, Budziszewska B (2015) Brain glucose metabolism in an animal model of depression. Neuroscience 295:198–208.

Dickens AM, Tovar YRLB, Yoo SW, Trout AL, Bae M, Kanmogne M, Megra B, Williams DW, Witwer KW, Gacias M, Tabatadze N, Cole RN, Casaccia P, Berman JW, Anthony DC, Haughey NJ (2017) Astrocyte-shed extracellular vesicles regulate the peripheral leukocyte response to inflammatory brain lesions. Sci Signal 10. doi: 10.1126/scisignal.aai7696.

Drysdale AT, et al. (2017) Resting-state connectivity biomarkers define neurophysiological subtypes of depression. Nat Med 23:28–38.

Edgar JR, Manna PT, Nishimura S, Banting G, Robinson MS (2016) Tetherin is an exosomal tether. Elife 5. doi: 10.7554/eLife.17180.

Girach F, Craig TJ, Rocca DL, Henley JM (2013) RIM1α sumoylation is required for fast synaptic vesicle exocytosis. Cell Rep 5:1294–1301.

Głombik K, Stachowicz A, Ślusarczyk J, Trojan E, Budziszewska B, Suski M, Kubera M, Lasoń W, Wędzony K, Olszanecki R, Basta-Kaim A (2015) Maternal stress predicts altered biogenesis and the profile of mitochondrial proteins in the frontal cortex and hippocampus of adult offspring rats. Psychoneuroendocrinology 60:151–162.

Głombik K, Stachowicz A, Trojan E, Olszanecki R, Ślusarczyk J, Suski M, Chamera K, Budziszewska B, Lasoń W, Basta-Kaim A (2017) Evaluation of the effectiveness of chronic antidepressant drug treatments in the hippocampal mitochondria - A proteomic study in an animal model of depression. Prog Neuropsychopharmacol Biol Psychiatry 78:51–60.

Goetzl EJ, Schwartz JB, Abner EL, Jicha GA, Kapogiannis D (2018) High complement levels in astrocyte-derived exosomes of alzheimer disease. Ann Neurol 83:544–552.

Hazelton I, Yates A, Dale A, Roodselaar J, Akbar N, Ruitenberg MJ, Anthony DC, Couch Y (2018) Exacerbation of acute traumatic brain injury by circulating extracellular vesicles. J Neurotrauma 35:639–651.

Kahne T, Richter S, Kolodziej A, Smalla KH, Pielot R, Engler A, Ohl FW, Dieterich DC, Seidenbecher C, Tischmeyer W, Naumann M, Gundelfinger ED (2016) Proteome rearrangements after auditory learning: high-resolution profiling of synapse-enriched protein fractions from mouse brain. J Neurochem 138:124–138.

Kolodziej A, Smalla KH, Richter S, Engler A, Pielot R, Dieterich DC, Tischmeyer W, Naumann M, Kahne T (2016) High resolution quantitative synaptic proteome profiling of mouse brain regions after auditory discrimination learning. J Vis Exp. doi: 10.3791/54992.

Koo JW, Russo SJ, Ferguson D, Nestler EJ, Duman RS (2010) Nuclear factor-kappab is a critical mediator of stress-impaired neurogenesis and depressive behavior. Proc Natl Acad Sci U S A 107:2669–2674.

Kowal J, Arras G, Colombo M, Jouve M, Morath JP, Primdal-Bengtson B, Dingli F, Loew D, Tkach M, Théry C (2016) Proteomic comparison defines novel markers to characterize heterogeneous populations of extracellular vesicle subtypes. Proc Natl Acad Sci U S A 113:E968–E977.

Krishnan V, Nestler EJ (2010) Linking molecules to mood: new insight into the biology of depression. Am J Psychiatry 167:1305–1320.

Kunadt M, et al. (2015) Extracellular vesicle sorting of α-synuclein is regulated by sumoylation. Acta Neuropathol 129:695–713.

Lener MS, Iosifescu DV (2015) In pursuit of neuroimaging biomarkers to guide treatment selection in major depressive disorder: a review of the literature. Ann N Y Acad Sci 1344:50–65.

Licinio J, Dong C, Wong ML (2009) Novel sequence variations in the brain-derived neurotrophic factor gene and association with major depression and antidepressant treatment response. Arch Gen Psychiatry 66:488–497.

Lin JY, Jiang MY, Kan ZM, Chu Y (2014) Influence of 5-HTR2A genetic polymorphisms on the efficacy of antidepressants in the treatment of major depressive disorder: a meta-analysis. J Affect Disord 168:430–438.

LoTurco J, Manent JB, Sidiqi F (2009) New and improved tools for in utero electroporation studies of developing cerebral cortex. Cereb Cortex 19:i120–i125.

Lv X, Si T, Wang G, Wang H, Liu Q, Hu C, Wang J, Su Y, Huang Y, Jiang H, Yu X (2016) The establishment of the objective diagnostic markers and personalized medical intervention in patients with major depressive disorder: rationale and protocol. BMC Psychiatry 16:240.

Maffioletti E, Cattaneo A, Rosso G, Maina G, Maj C, Gennarelli M, Tardito D, Bocchio-Chiavetto L (2016) Peripheral whole blood microRNA alterations in major depression and bipolar disorder. J Affect Disord 200:250–258.

Matsuzaki S, Lee L, Knock E, Srikumar T, Sakurai M, Hazrati LN, Katayama T, Staniszewski A, Raught B, Arancio O, Fraser PE (2015) SUMO1 affects synaptic function, spine density and memory. Sci Rep 5:10730.

Menard C, et al. (2017) Social stress induces neurovascular pathology promoting depression. Nat Neurosci 20:1752–1760.

Mustapic M, Eitan E, Werner JK Jr, Berkowitz ST, Lazaropoulos MP, Tran J, Goetzl EJ, Kapogiannis D (2017) Plasma extracellular vesicles enriched for neuronal origin: A potential window into brain pathologic processes. Front Neurosci 11:278.

Park SY, Choi JH, Ryu HS, Pak YK, Park KS, Lee HK, Lee W (2009) C1Q tumor necrosis factor alpha-related protein isoform 5 is increased in mitochondrial DNA-depleted myocytes and activates AMP-activated protein kinase. J Biol Chem 284:27780–27789.

Paul D, Baena V, Ge S, Jiang X, Jellison ER, Kiprono T, Agalliu D, Pachter JS (2016) Appearance of claudin-5+ leukocytes in the central nervous system during neuroinflammation: a novel role for endothelial-derived extracellular vesicles. J Neuroinflammation 13:292.

Pegtel DM, Peferoen L, Amor S (2014) Extracellular vesicles as modulators of cell-to-cell communication in the healthy and diseased brain. Philos Trans R Soc Lond B Biol Sci 369. doi: 10.1098/rstb.2013.0516.

Regenold WT, Pratt M, Nekkalapu S, Shapiro PS, Kristian T, Fiskum G (2012) Mitochondrial detachment of hexokinase 1 in mood and psychotic disorders: implications for brain energy metabolism and neurotrophic signaling. J Psychiatr Res 46:95–104.

Sandoval M, Luarte A, Herrera-Molina R, Varas-Godoy M, Santibanez M, Rubio FJ, Smit AB, Gundelfinger ED, Li KW, Smalla KH, Wyneken U (2013) The glycolytic enzyme aldolase C is up-regulated in rat forebrain microsomes and in the cerebrospinal fluid after repetitive fluoxetine treatment. Brain Res 1520:1–14.

Sántha P, Veszelka S, Hoyk Z, Mészáros M, Walter FR, Tóth AE, Kiss L, Kincses A, Oláh Z, Seprényi G, Rákhely G, Dér A, Pákáski M, Kálmán J, Kittel Á, Deli MA (2015) Restraint stress-induced morphological changes at the blood-brain barrier in adult rats. Front Mol Neurosci 8:88.

Shao H, Chung J, Balaj L, Charest A, Bigner DD, Carter BS, Hochberg FH, Breakefield XO, Weissleder R, Lee H (2012) Protein typing of circulating microvesicles allows real-time monitoring of glioblastoma therapy. Nat Med 18:1835–1840.

Sillitoe RV, Marzban H, Larouche M, Zahedi S, Affanni J, Hawkes R (2005) Conservation of the architecture of the anterior lobe vermis of the cerebellum across mammalian species. Prog Brain Res 148:283–297.

Siwek M, Sowa-Kućma M, Styczeń K, Misztak P, Nowak RJ, Szewczyk B, Dudek D, Rybakowski JK, Nowak G, Maes M (2017) Associations of serum cytokine receptor levels with melancholia, staging of illness, depressive and manic phases, and severity of depression in bipolar disorder. Mol Neurobiol 54:5883–5893.

Sokolova V, Ludwig AK, Hornung S, Rotan O, Horn PA, Epple M, Giebel B (2011) Characterisation of exosomes derived from human cells by nanoparticle tracking analysis and scanning electron microscopy. Colloids Surf B Biointerfaces 87:146–150.

Théry C, Amigorena S, Raposo G, Clayton A (2006) Isolation and characterization of exosomes from cell culture supernatants and biological fluids. Curr Protoc Cell Biol Chapter 3:Unit 3.22.

Torres-Platas SG, Nagy C, Wakid M, Turecki G, Mechawar N (2016) Glial fibrillary acidic protein is differentially expressed across cortical and subcortical regions in healthy brains and downregulated in the thalamus and caudate nucleus of depressed suicides. Mol Psychiatry 21:509–515.

Ventimiglia LN, Alonso MA (2016) Biogenesis and function of T cell-derived exosomes. Front Cell Dev Biol 4:84.

Villarroya-Beltri C, Baixauli F, Gutiérrez-Vázquez C, Sánchez-Madrid F, Mittelbrunn M (2014) Sorting it out: regulation of exosome loading. Semin Cancer Biol 28:3–13.

Vizcaíno JA, Csordas A, del-Toro N, Dianes JA, Griss J, Lavidas I, Mayer G, Perez-Riverol Y, Reisinger F, Ternent T, Xu QW, Wang R, Hermjakob H (2016) 2016 update of the PRIDE database and its related tools. Nucleic Acids Res 44:D447–D456.

Weckmann K, Deery MJ, Howard JA, Feret R, Asara JM, Dethloff F, Filiou MD, Iannace J, Labermaier C, Maccarrone G, Webhofer C, Teplytska L, Lilley K, Müller MB, Turck CW (2017) Ketamine's antidepressant effect is mediated by energy metabolism and antioxidant defense system. Sci Rep 7:15788.

Whittle N, Li L, Chen WQ, Yang JW, Sartori SB, Lubec G, Singewald N (2011) Changes in brain protein expression are linked to magnesium restriction-induced depression-like behavior. Amino Acids 40:1231–1248.

Willis CM, Ménoret A, Jellison ER, Nicaise AM, Vella AT, Crocker SJ (2017) A refined bead-free method to identify astrocytic exosomes in primary glial cultures and blood plasma. Front Neurosci 11:335.

Xue Y, Zhou F, Fu C, Xu Y, Yao X (2006) SUMOsp: a web server for sumoylation site prediction. Nucleic Acids Res 34:W254–W257.